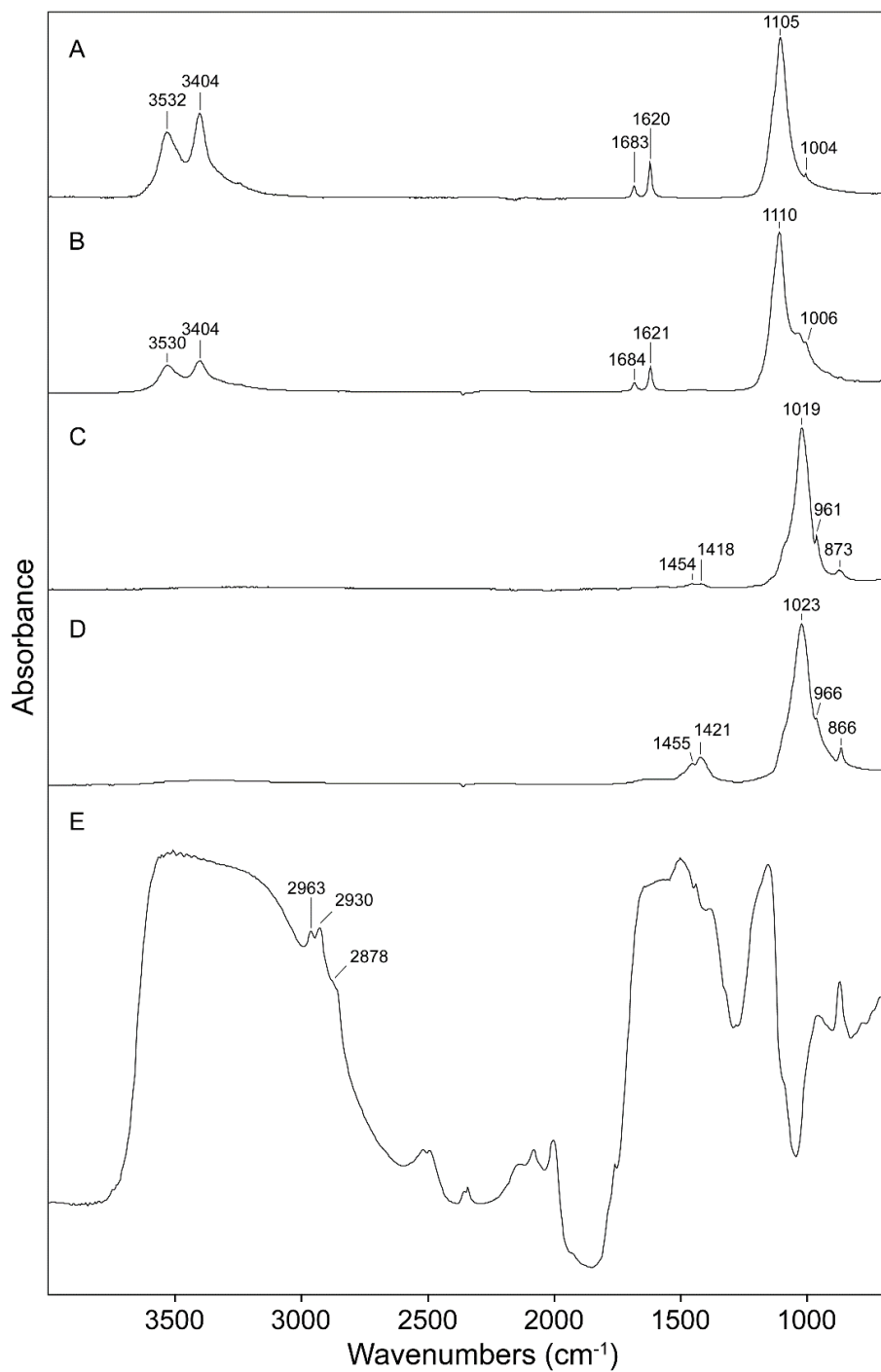
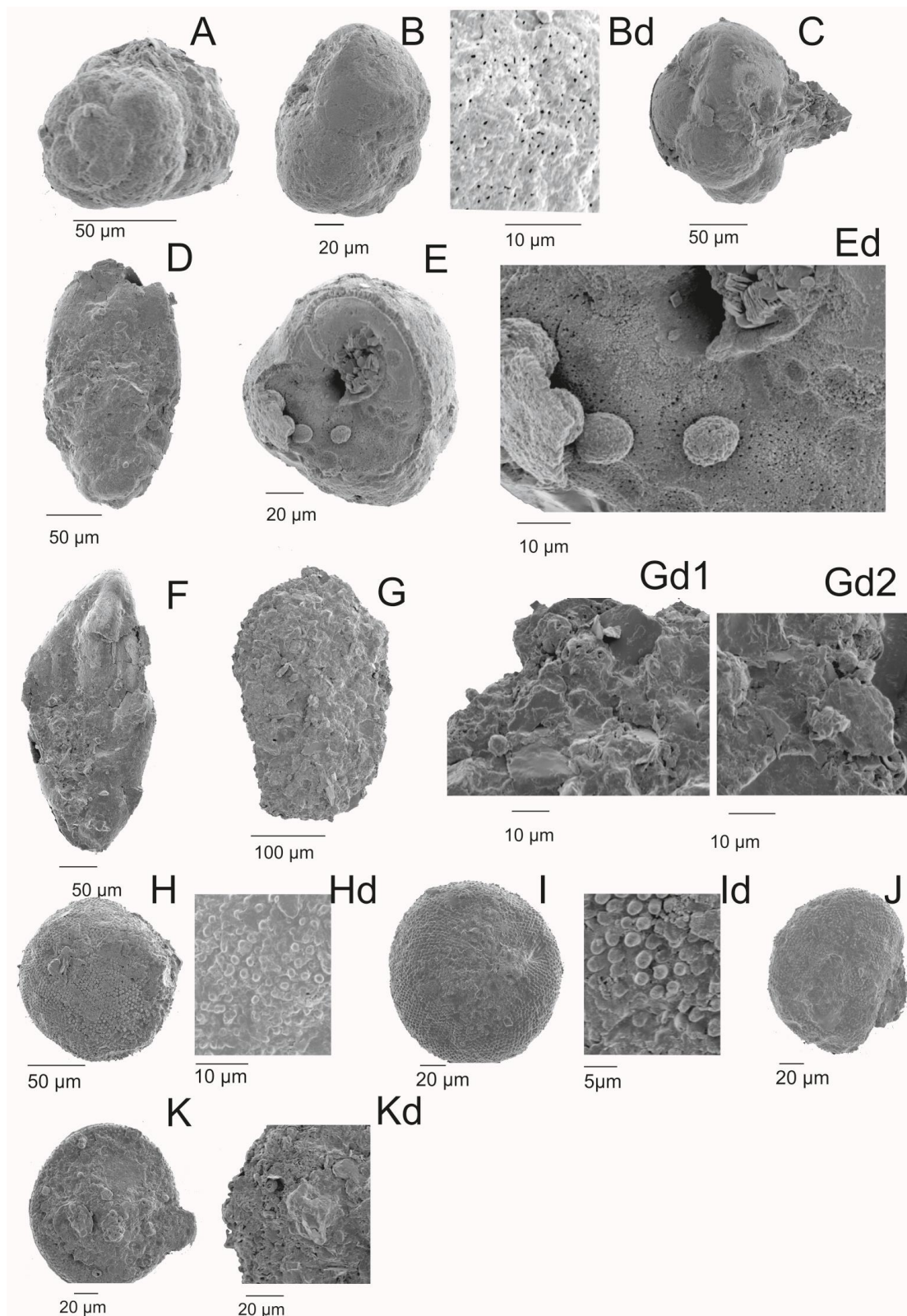


Supplementary Fig. 1. **a** Geographical position of the once existing Csillag-hegy brickyard (asterisk). **b** The surface outcrops of Oligocene formations surrounded by Eocene and Triassic rocks in the vicinity of the settlement Csillaghegy. The shorter and longer arrows mark the former outcrop of the the Kiscell Clay Fm. and Tard Clay Fm. (Csillag-hegy brickyard). 1) Oligocene Tard Clay Fm. (surface). 2) Oligocene Kiscell Clay Fm. (surface). 3) Oligocene Kiscell Clay Fm. (covered). 4) Eocene conglomerate, limestone with *Nummulites* or *Discocyliina*, bryozoan marl (surface). 5) Eocene conglomerate, limestone with *Nummulites* or *Discocyliina*, bryozoan marl (covered). 6) Eocene Buda Marl Fm. 7) Triassic grey dolomite (Hauptdolomite). 8) Triassic Diplopora Dolomite. **c** Geological profile of the former Csillag-hegy brickyard after⁷⁹. The exact level of the *Necroteuthis* specimens within the Tard Clay Fm. is unknown. 1) Kiscell Clay Fm., 2) travertine, 3) Tard Clay Fm., 4) Upper Eocene carbonates, 5) level with abundant shark teeth in the lower part of the Tard Clay Fm.



Supplementary Fig. 2. Recorded infrared spectra and reference spectra (Fourier-transform Infrared spectroscopy - FTIR). **a** reference spectrum of gypsum RRUFF R040029-1, **b** recorded spectrum of gypsum, **c** reference spectrum of (hydroxyl)apatite R050512-1, **d** recorded spectrum of (hydroxyl)apatite, **e** recorded spectrum of a mixture of fossilized/altered organic matter.



Supplementary Fig. 3. **a-e** *Caucasina* sp. cf. *Caucasina schischkinskayae* **bd** – detail of densely porous test. **d** Collapsed younger chambers in larger adult specimen. **e** Bacterial activity signs, inner septum with framboidal pyrite pseudomorphoses after bacteria (**ed**). **f** *Fursenkoina acuta* (compressed). **g** ?*Miliammina* sp. **gd1**, **gd2** Nannofossils incorporated into the test wall. **h-k** *Tasmanites* sp. **hd**, **id** Details of the external wall structure. **j** Inner cavity. **k**, **kd** Calcareous nannoplankton crust (integument) on the *Tasmanites* sp. wall.

Supplementary Micro CT imaging:

The micro-computed tomography images generated during and/or analysed during the current study are available in the figshare repository: <https://doi.org/10.6084/m9.figshare.13526024>⁹⁰. The *Necroteuthis* holotype which is the subject of the imaging is housed in the Hungarian Natural History Museum under item: No. M59/4672.

Supplementary Tables 1-3.

	Sample 1	Sample 2	Sample 3	Sample 4	Sample 5	
<i>Coccolithus pelagicus</i> (Wallich 1877) Schiller, 1930	11.18	36.07	56.99	43.00	32.73	NP2-Recent
<i>Coronocyclus nitescens</i> (Kamptner, 1963) Bramlette and Wilcoxon, 1967	0.74	0.00	0.00	2.00	0.00	NP15-NN6
<i>Coronocyclus nitescens</i> (Kamptner, 1963) Bramlette and Wilcoxon, 1967	0.00	0.00	1.08	0.00	0.00	NP15-NN6
<i>Cyclicargolithus floridanus</i> (Roth & Hay, in Hay et al., 1967) Bukry, 1971	2.94	1.64	0.00	1.00	0.91	NP15-NN7
<i>Discoaster nodifer</i> (Bramlette & Riedel, 1954) Bukry, 1973	0.74	0.00	0.00	0.00	0.00	NP14-NP23
<i>Helicosphaera bipuncta</i> de Kaenel & Bergen, in Boesiger et al. 2017	0.93	0.00	0.00	2.00	0.91	NP22-NN4
<i>Pontosphaera enormis</i> (Locker, 1967) Perch-Nielsen, 1984	0.52	0.00	0.00	0.00	0.00	NP10-NP25
<i>Pontosphaera latielectica</i> (Baldi-Beke, in Baldi-Beke & Baldi 1974) Perch-Nielsen 1984	1.47	0.00	0.00	1.00	1.82	NP10-NP24
<i>Reticulofenestra bisecta</i> (Hay, Mohler and Wade, 1966) Roth, 1970	0.00	0.00	0.85	0.00	0.00	NP17-NN1
<i>Reticulofenestra daviesii</i> (Haq, 1968) Haq, 1971	0.74	0.92	1.30	4.00	0.91	NP14-NN2
<i>Reticulofenestra lockeri</i> Müller, 1970	8.54	6.56	0.00	20.00	18.18	NP17-NN2
<i>Reticulofenestra minuta</i> Roth, 1970	5.88	2.36	0.00	2.00	0.00	NP13-NN16
<i>Reticulofenestra ornata</i> Müller 1970	65.44	52.46	38.71	20.00	40.91	NP22-NP24
<i>Reticulofenestra umbilicus</i> (Levin, 1965) Martini & Ritzkowski, 1968	0.00	0.00	0.00	0.00	1.82	NP16--NP22
<i>Sphenolithus moriformis</i> (Brönnimann & Stradner, 1960) Bramlette & Wilcoxon, 1967	0.00	0.00	0.00	0.00	0.91	NP5-NN15
<i>Sphenolithus pseudoradians</i> Bramlette & Wilcoxon, 1967	0.89	0.00	0.00	0.00	0.00	NP15-NP24
<i>Syracosphaera</i> sp.	0.00	0.00	0.00	5.00	0.91	
<i>Thoracosphaera</i> sp.	0.00	0.00	1.08	0.00	0.00	

Supplementary Table 1: Diversity, abundance and stratigraphic distribution of calcareous nannofossils recorded from *Necroteuthis*-bearing sediment.

locality	No. level	sample	$\delta^{13}\text{C}_{\text{carb}}$	$\delta^{18}\text{O}_{\text{carb}}$	StDev C	StDev O
Csillaghegy	JS1	2622.15	-2.27	-5.87	0.011	0.022
Csillaghegy	JS2	3031.32	-2.46	-6.01	0.010	0.014
Csillaghegy	JS3	2444.14	-2.38	-5.39	0.011	0.029
Csillaghegy	JS4	4228.73	-2.41	-5.74	0.016	0.020
Csillaghegy	JS5	2781.15	-2.34	-5.64	0.008	0.030
Csillaghegy	JS6	2394.42	-2.50	-5.72	0.006	0.010
Csillaghegy	JS7	1428.39	-2.50	-5.56	0.009	0.013
Csillaghegy	JS8	2325.24	-2.49	-5.58	0.013	0.035
Csillaghegy	JS9	4039.36	-2.45	-5.15	0.008	0.005
Csillaghegy	JS10	3751.30	-2.45	-5.38	0.011	0.013
Csillaghegy	JS11	3440.80	-2.59	-5.57	0.008	0.013
Csillaghegy	JS12	3051.95	-2.40	-5.32	0.017	0.011
Csillaghegy	JS13	2003.81	-2.61	-6.13	0.016	0.016
Csillaghegy	JS14	1846.05	-3.25	-5.92	0.020	0.025
Csillaghegy	JS15	1802.10	-2.48	-5.39	0.026	0.023
Csillaghegy	JS16	1891.25	-2.45	-5.49	0.032	0.036
Csillaghegy	JS17	3066.10	-0.93	-2.73	0.041	0.028
Csillaghegy	JS18	3190.09	-0.98	-2.01	0.022	0.039
Csillaghegy	JS19	3646.33	-1.08	-1.99	0.022	0.013

Supplementary Table 2: Table of measured stable isotopes $\delta^{13}\text{C}_{\text{carb}}$ and $\delta^{18}\text{O}_{\text{carb}}$ from the bulk rock of *Necroteuthis*-bearing specimen (blue – Tard Clay Fm.) and overlying Kiscell Clay Fm. yielding *Archaeosepia* cuttlebones (green). Level with gladius highlighted by grey.

No. analysis	No. Peak	Nr	Rt	Ampl 44	BGD 44	Area All	$\delta^{13}\text{C}/\delta^{12}\text{C}$	$\delta^{13}\text{C}_{\text{org}}$
82009	JS1	3	165.9	3841	10.9	71.768	-26.7229	-26.75
82010	JS2	3	165.1	3467	10.4	64.622	-26.6731	-26.72
82011	JS3	3	165.3	4211	10.6	78.555	-26.8036	-26.80
82012	JS4	3	165.1	3698	10.7	69.137	-26.7638	-26.76
82013	JS5	3	165.5	3303	10.6	62.035	-26.8126	-26.81
82014		3	165.3	3800	10.3	71.299	-26.8724	-26.87
82015	JS7	3	165.1	3406	10.7	63.637	-26.9282	-26.93
82016	JS8	3	165.1	3752	10.8	70.184	-27.0627	-27.06
82017	JS9	3	165.3	3500	10.2	65.3	-26.6372	-26.64
82018	JS10	3	165.3	3346	10.2	62.783	-26.8007	-26.80
82019	JS11	3	165.5	3264	10.0	61.167	-26.7319	-26.73
82020	JS12	3	164.7	3748	10.4	69.712	-26.7389	-26.74
82021	JS13	3	164.9	3274	10.4	60.656	-26.7269	-26.73
82022	JS14	3	165.5	3181	10.1	60.768	-26.4558	-26.46
82023	JS15	3	165.7	4118	10.2	77.684	-27.0697	-27.07
82024	JS16	3	164.9	3387	10.5	63.312	-26.8644	-26.86
82025	JS1	3	165.3	4188	10.3	78.645	-26.7678	control
82026	JS2	3	165.3	4046	10.0	75.666	-26.7638	control

Supplementary Table 3: Table of measured stable isotope $\delta^{13}\text{C}_{\text{org}}$ from the bulk rock of *Necroteuthis*-bearing specimen. Level with gladius highlighted by grey.